

## The effects of $Mg_2Si_{(p)}$ on microstructure and mechanical properties of AA332 composite

Fizam Zainon<sup>1a</sup>, Khairrel Rafezi Ahmad<sup>\*2</sup> and Ruslizam Daud<sup>1b</sup>

<sup>1</sup>Fracture and Damage Research Group, School of Mechatronic Engineering,  
Pauh Putra Campus, Universiti Malaysia Perlis, 02600 Arau, Perlis, Malaysia

<sup>2</sup>Electrochemistry of Green Materials Research Group, Center of Excellence Geopolymer & Green Technology  
(CEGeoGTech), School of Materials Engineering,  
Universiti Malaysia Perlis, 02600 Jejawi, Arau, Perlis, Malaysia

(Received January 27, 2016, Revised June 27, 2016, Accepted June 28, 2016)

**Abstract.** This paper describes a study on the effects of  $Mg_2Si_{(p)}$  addition on the microstructure, porosity, and mechanical properties namely hardness and tensile properties of AA332 composite. Each composite respectively contains 5, 10, 15, and 20 wt% reinforcement particles developed by a stir-casting. The molten composite was stirred at 600 rpm and melted at  $900^\circ C \pm 5^\circ C$ . The  $Mg_2Si$  particles were wrapped in an aluminum foil to keep them from burning when melting. The findings revealed that the microstructure of  $Mg_2Si_{(p)}/AA332$  consists of  $\alpha$ -Al, binary eutectic (Al+ $Mg_2Si$ ),  $Mg_2Si$  particles, and intermetallic compound. The intermetallic compound was identified as Fe-rich and Cu-rich, formed as polygonal or blocky, Chinese script, needle-like, and polyhedrons or “skeleton like”. The porosity of  $Mg_2Si_{(p)}/AA332$  composite increased from 8-10% and the density decreased from 9-12% from as-cast. Mechanical properties such as hardness increased for over 42% from as-cast and the highest UTS, elongation, and maximum Q.I were achieved in the sample of 10%  $Mg_2Si$ . The study concludes that combined with AA332, the amount of 10 wt% of  $Mg_2Si$  is a suitable reinforcement quantity with the combination of AA332.

**Keywords:** Aluminum Matrix Composite (AMCs);  $Mg_2Si$ ; intermetallic; microstructure; mechanical properties

### 1. Introduction

Automotive parts made of cast iron have been replaced with composite components which can contribute to higher fuel efficiency and lower levels of emissions (Okayasu *et al.* 2012). These composite components can significantly increase fuel efficiency of vehicles by reducing vehicle weight by 60% (Williams 2012). They can also reduce  $CO_2$  emission and improve the environment due to proper use of fuel (Pardeep *et al.* 2013).

$Mg_2Si/Al$ -Si composite is a potential material for automobile because  $Mg_2Si$  is a hard intermetallic compound with a high melting point ( $1085^\circ C$ ), low density ( $1.88g/cm^3$ ), low

---

\*Corresponding author, Ph.D., E-mail: [rafezi@unimap.edu.my](mailto:rafezi@unimap.edu.my)

<sup>a</sup>Ph.D. Student, E-mail: [anna.nocah@gmail.com](mailto:anna.nocah@gmail.com)

<sup>b</sup>Ph.D., E-mail: [ruslizam@unimap.edu.my](mailto:ruslizam@unimap.edu.my)

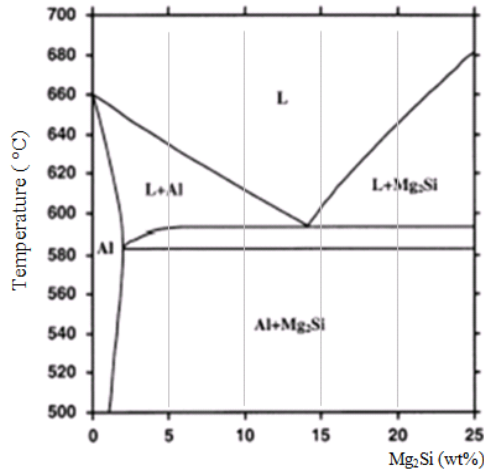
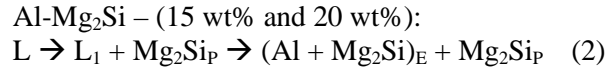
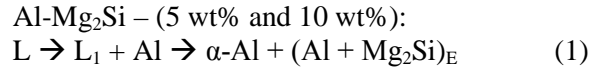


Fig. 1 Equilibrium phase diagram of the pseudo-binary Al-Mg<sub>2</sub>Si



where  $P$  is primary particle and  $E$  is eutectic

coefficient of thermal expansion ( $7.5 \times 10^{-6} \text{ K}^{-1}$ ), 120 GPa of Young's modulus, and high micro Vicker's hardness. These characteristics make Mg<sub>2</sub>Si suitable to be reinforced in matrix alloy (Ajith Kumar *et al.* 2013; Aydin and Findik 2010; Emamy *et al.* 2013a; Nasiri *et al.* 2012; Qingxiu *et al.* 2009; Soltani *et al.* 2014; Tang *et al.* 2011; and Wu *et al.* 2013). In fact in Hadian *et al.* (2009) study, they identified that Mg<sub>2</sub>Si particles exhibit low equilibrium interface and rough morphology, which create an effect of low ductility in matrix alloy. Nasiri *et al.* (2012) also agreed that Al-Mg<sub>2</sub>Si composites are excellent materials to replace Al-Si alloy or Al-SiC composites.

As shown in the binary Al- Mg<sub>2</sub>Si system (Fig. 1), the grey lines represent the composites alloy investigated in this study. During the solidification process, Mg<sub>2</sub>Si particles are formed as primary Mg<sub>2</sub>Si<sub>P</sub>. Al with Mg<sub>2</sub>Si will co-solidify from the liquid alloy to a ternary phase area, forming a binary eutectic reaction. Hence increasing Mg<sub>2</sub>Si will change the equilibrium solidification paths as shown in Eqs. (1)-(2).

Among the various Mg<sub>2</sub>Si/Al composite fabricating methods, stir-casting has recently attracted considerable attention for its compatible interfaces and thermodynamically stable property (Qingxiu *et al.* 2009). The stir-casting process is also widely accepted in industries due to lower production costs, simplicity, flexibility, and applicability to large quantity production (Panwar and Pandey 2013; Valibeygloo *et al.* 2013). The process also requires shorter processing period (Hamedan and Shahmiri 2012). Given these points there is a need to use a stir-casting method to develop a composite from Mg<sub>2</sub>Si/Al that are lighter and with excellent mechanical properties.

In a study on *in-situ* Mg<sub>2</sub>Si/Al-Si composite with different compositions, Qingxiu *et al.* (2009) also recommended an *in-situ* casting method to fabricate Mg<sub>2</sub>Si/Al-Si composite. The authors identified that the amount of Mg<sub>2</sub>Si increased as Mg content increased. The morphology changed from undeveloped to developed Chinese script-like particles, and finally irregular Mg<sub>2</sub>Si particles appeared. Meanwhile, the hardness and tensile strength of the cast *in-situ* Mg<sub>2</sub>Si/Al-Si composite did not increase as Mg content increased, but were related to the size and morphology of the eutectic Mg<sub>2</sub>Si phases and primary Mg<sub>2</sub>Si.

Liu *et al.* (2011) study, they investigated the effect of Mg<sub>2</sub>Si contents on the microstructure of Mg<sub>2</sub>Si particle reinforced in hypereutectic Al-Si alloy composite. The hypereutectic Al-Si alloy

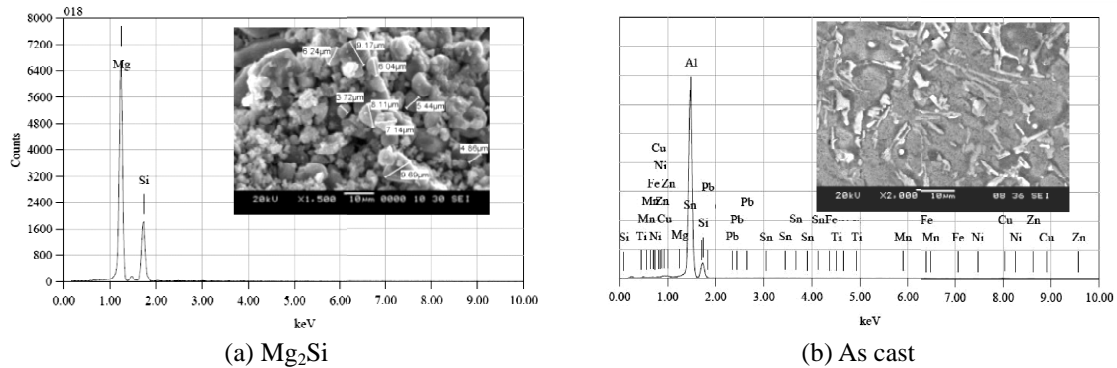


Fig. 2 EDX spectrum and SEM micrograph

contained about 19.7% Si, and 6.4-12.7% Mg was added with 10, 12, 15, 18, and 20% of  $Mg_2Si$  particles. The authors argued that the microstructures of the composite consist of  $\alpha$ -Al, primary  $Mg_2Si$ , and primary Si. The morphology of  $Mg_2Si$  evidently changed as the content of  $Mg_2Si$  increased. As reported, the morphology of 10-12%  $Mg_2Si$  presented a polygon-like, 15% of  $Mg_2Si$  presented a cross-like, and 18% and 20% of  $Mg_2Si$ , formed a coarse, dendritic-like particles. Coarse  $Mg_2Si$  particles could delay the solidification time. The authors also reported that the prolonged melting time had developed coarse, dendritic-like particles because  $Mg_2Si$  had enough time to grow up. Hence they concluded that the size of  $Mg_2Si$  is directly connected to the development of  $Mg_2Si$  nuclei.

In another study, Emamy *et al.* (2013) investigated the effect of hot extrusion process on the microstructures and tensile properties of aluminum matrix. The authors reported that the microstructures consist of  $\alpha$ -Al, primary  $Mg_2Si$  particles, and Al- $Mg_2Si$  eutectic. The primary  $Mg_2Si$  particles were formed in the matrix of Al- $Mg_2Si$  eutectic. The authors identified that the morphology of primary  $Mg_2Si$  particles increased and formed irregular and dendritic particles when the amount of  $Mg_2Si$  increased in the system. Meanwhile, the Al- $Mg_2Si$  eutectic was considerably reduced. The authors concluded that by increasing the amount of  $Mg_2Si$ , the average size and volume fraction of primary  $Mg_2Si$  particles increased drastically. In this study, the objective is to investigate the microstructural and mechanical properties of  $Mg_2Si_p/AA332$  with different weight percentages of reinforcement.

## 2. Experimental procedure

Aluminum alloy AA332 was used as matrix material and  $Mg_2Si$  with particle size of  $\leq 10\mu m$  was used as reinforcement. Fig. 2(a) shows the particle size and the EDX spectrum of  $Mg_2Si$  and Fig. 2(b) shows the SEM micrograph and the EDX spectrum of as-cast. Each composite respectively contained 5, 10, 15, and 20 wt% reinforcement particles developed by a stir-casting method. First, the  $Mg_2Si$  particles were preheated in an electrical oven at  $200^\circ C$  for 2 hours to (1) eliminate moisture and other unstable substances and (2) improve the particles' wettability in an atmospheric condition. All  $Mg_2Si$  particles were wrapped in an aluminum foil to keep them from burning at melt surface during the mixing process.

The AA332 ingot was melted in a graphite crucible in a chamber furnace at  $900^\circ C \pm 5^\circ C$  for 45

Table 1 Chemical composition of as-cast and Mg<sub>2</sub>Si<sub>(p)</sub>/AA332 composite

	Si	Fe	Cu	Mn	Mg	Ni	Zn	Ti	Pb	Sn	Al
As cast	11.09	0.94	1.63	0.21	0.27	0.07	0.98	0.05	0.04	0.02	rest
5% Mg <sub>2</sub> Si	11.44	0.90	1.68	0.19	0.91	0.07	0.89	0.05	0.05	0.02	rest
10% Mg <sub>2</sub> Si	10.89	1.23	1.81	0.20	1.88	0.11	0.95	0.05	0.08	0.02	rest
15% Mg <sub>2</sub> Si	11.01	1.43	1.63	0.22	3.44	0.11	0.92	0.05	0.08	0.02	rest
20% Mg <sub>2</sub> Si	10.79	1.55	1.71	0.21	3.56	0.13	0.90	0.05	0.06	0.02	rest

minutes. The fully molten alloy was then stirred at 600 rpm to form the vortex in the melted alloy. Once the vortex was formed, the Mg<sub>2</sub>Si particles were added and the stirring continued for 20 minutes. The molten alloy was then re-melted at 900°C ± 5°C for another 15 minutes in the same furnace to ensure that the distribution of homogeneous particles melted evenly. Finally, the molten alloy was casted into a heated graphite crucible mould (200°C) to produce samples of 150mm length and 10mm diameter, which were further set to solidify at room temperature.

Their chemical compositions were analysed using an optical emission spectrometer (Q8 MAGELLAN) metal analysis tester. The chemical compositions of as-cast and Mg<sub>2</sub>Si<sub>(p)</sub>/AA332 composite are shown in Table 1. The morphology of the samples was observed using an optical microscope (Olympus, BX41M) equipped with a digital camera (PowerShot A460). The image was analysed using Image J software. Scanning Electron Micrographs (SEM) JEOL JSM-6064 LA equipped with an Energy Dispersive X-ray Spectroscopy (EDX) were used to identify the as-cast phase of the morphology.

The bulk density of the samples was measured by using a pycnometer gas displacement density analyser (Micromeritics AccuPyc II 1340). Inert gas (helium) was used as the medium and all samples were verified for 10 purges for one cycle. Based on the density measurement, the percentage of porosity of the composites was calculated using Eq. (3)

$$\% \text{ Porosity } , \theta = \left[ 1 - \frac{\rho_c}{\rho_m(1 - W_p) + \rho_p W_p} \right] \times 100 \quad (3)$$

Where  $\rho$  is density in g/cm<sup>3</sup>,  $W$  is the volume fraction of reinforcement particulates,  $c$ ,  $m$ , and  $p$  is the composite, matrix, and reinforcement.

Next, hardness analysis was performed using Vicker's hardness tester (FV-700e) by following the ASTM International E384-11. Using a tensile testing machine, tensile tests were performed for the samples at room temperature according to ASTM International E8/E8M-13a standard. The test speed used was 1mm/min and the strain was measured with a 25mm extensometer. The tensile tests were carried out to obtain the ultimate tensile strength (UTS) and elongation to fracture (El).

### 3. Result and discussion

#### 3.1 Morphology

Fig. 3 shows the characteristics of the microstructures of as-cast and Mg<sub>2</sub>Si<sub>(p)</sub>/AA332 composite. Fig. 3(a) shows the structure of as cast, whereas contains with  $\alpha$ -Al, Si particles, and eutectic Si. The dendritic of  $\alpha$ -Al was formed in equiaxed grain and was dominant in the

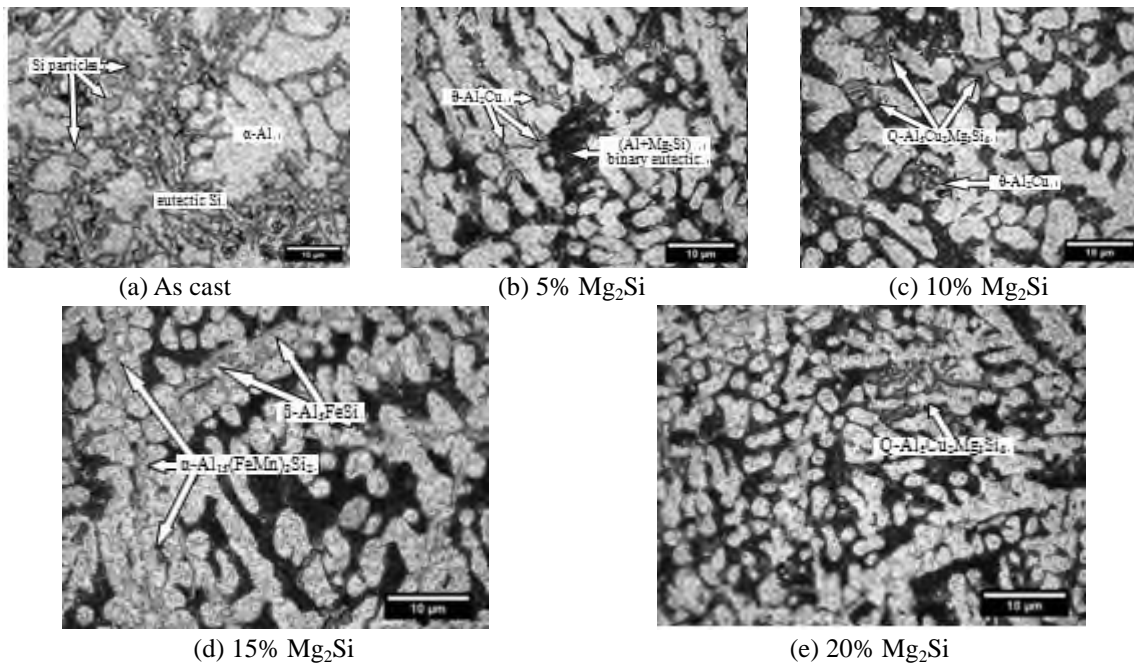


Fig. 3 Optical micrograph of as cast and  $Mg_2Si_{(p)}$ /AA332 composite

microstructures. As shown in the figure, the eutectic Si continued along the  $\alpha$ -Al grain boundaries while the Si particles appeared in polyhedral or blocky shape. Zeren (2007) concluded that Al-Si alloy contains two kinds of Si phase: plate-like eutectic Si and coarse, primary Si particles. Similarly, the microstructures of Al-Si alloy commonly depend on the nucleation and cooling rate during solidification. They also consist of coarse and segregated Si particles along with needle-like eutectic (Vijeesh and Narayan 2014). With exceptional castability and wear-resistance properties, the eutectic Al-Si alloys are favourable for manufacturing pistons and other critical components.

Figs. 3(b)-(e) shows the microstructures of  $Mg_2Si_{(p)}$ /AA332 composite. As shown in the Al- $Mg_2Si$  phase diagram (Fig. 1) and equilibrium solidification (Eqs. (1)–(2)), the microstructures of  $Mg_2Si_{(p)}$ /AA332 composite consisted of  $\alpha$ -Al, binary eutectic (Al+ $Mg_2Si$ ),  $Mg_2Si$  particles, and intermetallic compound. It can be observed that  $\alpha$ -Al was formed into the cell structure. Clearly the size of  $\alpha$ -Al has decreased and become spherical with the increase of  $Mg_2Si$  content.

The identification of intermetallic phases is a significant part of complex compositions. A range of different intermetallic phases are formed during a solidification process and this depends on the composition of alloy and the condition of crystallisation. Different intermetallic phases constitute various shapes of particles such as needle-like, plate-like, polygonal and “Chinese script”. In terms of size and distribution, it can be located at the grain boundaries and may form a dendritic network structure (Mrowka-Nowotnik 2011). The presence of additional elements in AA332 alloy allows many complex intermetallic phases to form such as binary, ternary, and quaternary phases. According to Belov *et al.* (2005), the quaternary systems of Al-Cu-Fe-Mg-Ni-Si will form the phases such as  $\epsilon$ ,  $\theta$ , M,  $\delta$ ,  $\gamma$ , T,  $\beta$ ,  $\pi$ , and Q.

The appearance of intermetallic can be observed in Figs. 3(b)-(e) and Figs. 4(a)-(d). In this case, the intermetallic compounds were identified as  $\theta$ -Al<sub>2</sub>Cu, Q-Al<sub>5</sub>Cu<sub>2</sub>Mg<sub>3</sub>Si<sub>6</sub>,  $\beta$ -Al<sub>3</sub>FeSi, and

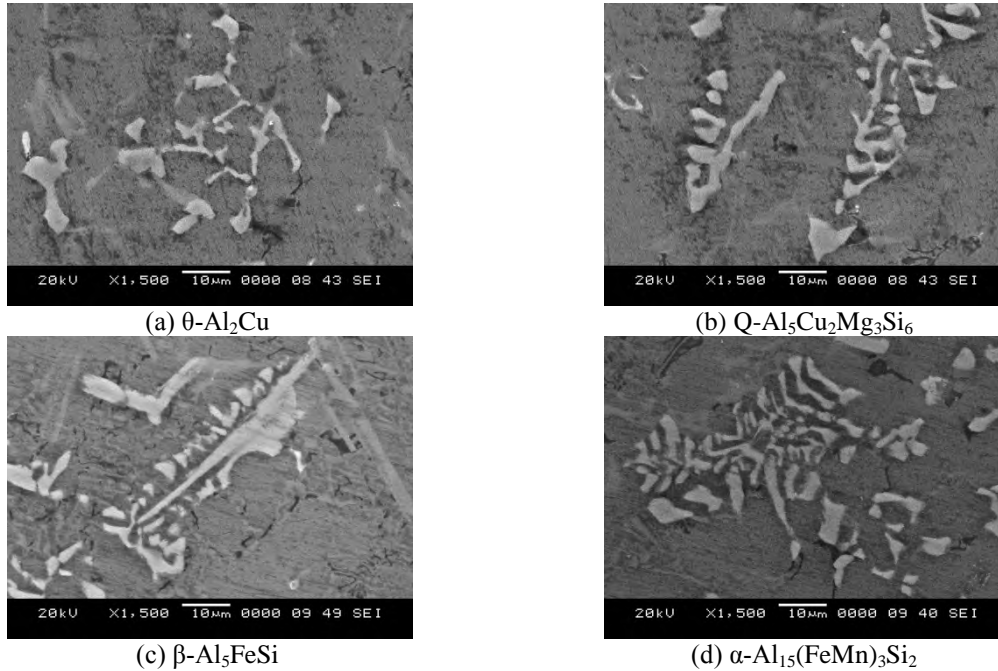


Fig. 4 The intermetallic precipitation of  $Mg_2Si_{(p)}$ /AA332 composite

$\alpha-Al_{15}(FeMn)_3Si_2$ . Figs. 3(b), (c), and (e) show the deformation of each  $\theta-Al_2Cu$  and  $Q-Al_5Cu_2Mg_3Si_6$  intermetallic phase. Clearly seen in Figs. 4(a)–(b),  $\theta-Al_2Cu$  was formed in a polygonal or blocky shape; while  $Q-Al_5Cu_2Mg_3Si_6$  appeared as “Chinese script.” As known, Cu produces  $Q-Al_5Cu_2Mg_3Si_6$  and  $\theta-Al_2Cu$  precipitates. This process increases the overall matrix strength by a mechanism called a precipitation strengthening effect. During solidification,  $\theta-Al_2Cu$  phase is formed because Cu is segregated from its liquid form (Samuel *et al.* 2014). This concentration increases with the solid fraction. Subsequently, during the final phase of the solidification process, the precipitation of  $Q-Al_5Cu_2Mg_3Si_6$  developed from the  $\theta-Al_2Cu$  phase. An investigation by Farkoosh and Pekguleryuz (2015) reported that by increasing the Mg level, the amount of  $Q-Al_5Cu_2Mg_3Si_6$  will increase and the amount of  $\theta-Al_2Cu$  will diminish. This can be seen from Figs. 3(c) and (e) when the Mg content increased from 1.88 wt% to 3.56 wt% (Table 1).

The reaction of Mg or Mn with Fe in the cast alloy has formed Fe-rich intermetallic compounds. These Fe-rich intermetallic compounds appear in the microstructures of various forms after a casting process, depending on the amount of Mg or Mn (Yildirim and Ozyurek 2013). As seen in Fig. 3(d) and Figs. 4(c)–(d), the intermetallic of  $\beta-Al_5FeSi$  and  $\alpha-Al_{15}(FeMn)_3Si_2$  appeared as needle-like and polyhedrons (Samuel *et al.*, 2014) or “skeleton-like” (Hurtalova *et al.*, 2012) respectively. Generally, the phase of  $\beta-Al_5FeSi$  precipitates in the inter-dendritic and intergranular regions as platelets (Hurtalova *et al.* 2012). The intermetallic of  $\beta-Al_5FeSi$  can be transformed into  $\pi-Al_9FeMg_3Si_5$  when the Mg increases and the Mn content may be reduced during the  $\beta-Al_5FeSi$  phase and promote the formation of  $\alpha-Al_{15}(FeMn)_3Si_2$ . This  $\beta-Al_5FeSi$  phase is detrimental because it affects high-stress concentrations, increases crack imitation, and decreases ductility. However, these effects can be reduced by increasing the cooling rate or by superheating the molten metal.

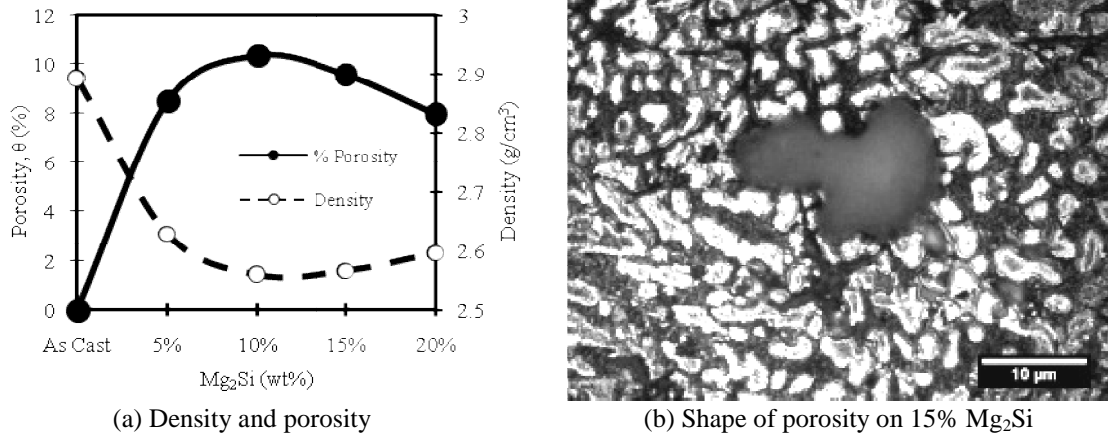


Fig. 5 Density and porosity of  $Mg_2Si_{(p)}/AA332$  composite

Samuel *et al.* (2014) reported that an  $\alpha-Al_{15}(FeMn)_3Si_2$  phase occurs during eutectic solidification with  $\alpha-Al$ . This will appear as polyhedrons if it solidifies before the eutectic reaction. Usually, the formation of  $\alpha-Al_{15}(FeMn)_3Si_2$  does not initiate porosity like the  $\beta-Al_5FeSi$  phase. However, as reported by Yildirim and Ozyurek (2013) and Hurtalova *et al.* (2012), Fe-rich intermetallic compounds reduce the mechanical properties of alloy such as tensile properties and ductility.

### 3.2 Density and porosity

In Fig. 5, the density and porosity of as-cast and  $Mg_2Si_{(p)}/AA332$  composite with different amounts are given. The optical micrograph of the porosity shape is also displayed. In Fig. 5(a), the porosity of the  $Mg_2Si_{(p)}/AA332$  composite increased from 8 - 10% from as-cast while the density decreased in parallel with the increasing of  $Mg_2Si$ . Compared to as-cast, the density of  $Mg_2Si_{(p)}/AA332$  composite decreased between 9 - 12%. Low density was detected for sample containing 10%  $Mg_2Si$ . This can be attributed to the high porosity volume within the sample.

Numerous parameters may affect the formation of porosity such as the presence of water vapour on the reinforcement surfaces and hydrogen gas (Muhammad Faisal Alam 2013), the effect of cooling rate (Hosseini *et al.* 2013), the increase of modifiers and alloying elements, and the presence of  $\beta-Al_5FeSi$  intermetallic phase (Hurtalova *et al.* 2012).

Taylor (2012) agreed that Fe has the potential to form porosity at high-iron levels. Additionally, Ammar *et al.* (2008) reported that Fe has a strong influence on porosity in Al-Si-Cu alloy. It changes the pore morphology from discrete, isolated pores to spongy, inter-dendritic pores. Moreover, Hurtalova *et al.* (2012) noted that the dominant Fe-rich phase shape of  $\beta-Al_5FeSi$  can adversely affect the mechanical properties and lead to the formation of excessive shrinkage porosity. As shown in Fig. 5(b) and Fig. 3(d), the porosity in 15%  $Mg_2Si$  occurred because of Fe-rich intermetallic. In this sense, porosity can be avoided by removing the oxygen prior to the solidification or by making sure it does not re-emerge as gas (Black and Kohser 2008). Black and Kohser (2008) specifically mentioned that the solidification process is expected to be properly designed so that it can take place without producing internal porosity. Additionally, the design of such mould in the gating system also influences the casting condition, known for its influence on

the solidification and feeding condition of the melt (Ammar *et al.* 2008).

In most cases, die casting, stir casting, and gravity casting techniques are prone to higher porosity compared to other casting methods due to the entrapment of air bubbles during the turbulent filling of the die cavity (Garza-Delgado 2007; Sajjadi *et al.* 2012; and Sekar *et al.* 2013). For the solution, the use of intensification pressure helps in reducing porosity levels as well as in feeding material to complex regions. The porosity content in compo casting is also lower due to good wettability of particles (Sajjadi *et al.* 2012). Other than that, Sekar *et al.* (2013) and Dhanashekar and Kumar (2014) reported that the components produced by squeeze casting can avoid gas porosity or shrinkage porosity. A secondary processing method such as shape casting, forging, extrusion, or a heat treatment method can be implemented to reduce porosity (Muhammad Faisal Alam 2013).

A stirring process can bring air into a molten whereas the stirring speed, size, and position of the impeller can significantly affect the porosity of a material (Qiang 2009). Besides that, Yu (2010) suggested using electromagnetic stirring to refine internal structures, reduce porosity, and minimise internal cracks. Also, porosity can be reduced by using high cooling rates during solidification. Accordingly, Hosseini *et al.* (2013) confirmed that a high cooling rate reduces shrinkage porosity and causes more uniform distribution of porosity. As shown in Fig. 5(b), the shrinkage porosity occurred during the process of solidification. This is because the pores are determined by the angular or elongate with a dendritic structure inside. The shrinkage porosity also occurred due to non-uniform solidification of the material, which actually attempts to tear itself to pieces as it solidifies (Mitrasinovic 2004).

### 3.3 Hardness

Fig. 6 depicts the micro-hardness resulting from the as-cast and  $Mg_2Si_{(p)}/AA332$  composite. Before reinforcement, the hardness for as-cast recorded 95.36Hv. The hardness of  $Mg_2Si_{(p)}/AA332$  composite had a significant increase from 42% to 53% from as-cast. In this study, the sample of 5%  $Mg_2Si$  recorded the highest hardness (53.3%) while the sample of 15%  $Mg_2Si$  recorded the lowest hardness.

The reinforcement of  $Mg_2Si$  particles had improved the micro-hardness of composites in comparison to the unreinforced matrix. In this case, alterations in the morphology of Fe-rich and

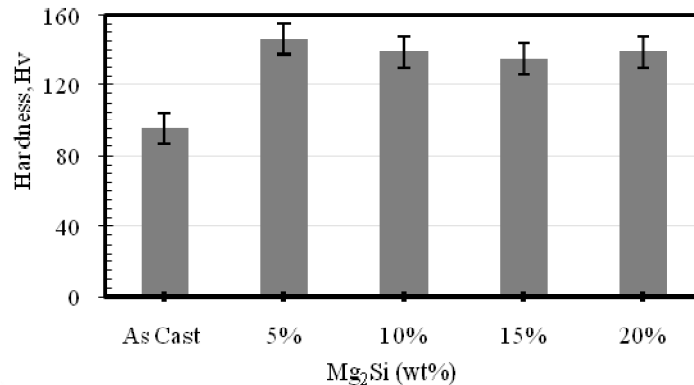


Fig. 6 The micro-hardness of as-cast and  $Mg_2Si_{(p)}/AA332$  composite

Cu-rich intermetallic phase have changed the mechanical properties of the composites (Hurtalova *et al.*, 2012). Therefore, the development of intermetallic such as  $\beta-Al_5FeSi$ ,  $\alpha-Al_{15}(FeMn)_3Si_2$ ,  $\theta-Al_2Cu$ , and  $Q-Al_5Cu_2Mg_3Si_6$  in the  $Mg_2Si_{(p)}/AA332$  composite microstructure (Fig. 3) was the causal factor of hardness enhancement. As reported by Emamy *et al.* (2013), the presence of hard intermetallic in a matrix is expected to increase a mechanical properties. Thus these intermetallic compounds are assumed to be strong reinforcement in the composite.

The dissimilarity in hardness between  $Mg_2Si_{(p)}/AA332$  composite can be attributed to the distribution of  $Mg_2Si$  particles during solidification and the percentage of  $Mg_2Si$  particles added into the matrix. Size reduction, better distribution of primary  $Mg_2Si$  particles, reduction in cluster regions, as well as porosity reduction in matrix and fracture are also attributed to the hardness difference in composite (Soltani *et al.* 2014). As shown in Fig. 5(a), higher porosity defects were observed in samples of 10%  $Mg_2Si$  and 15%  $Mg_2Si$ . The hardness of these samples are slightly lower than that of other samples. On the other hand, the mechanical properties of  $Mg_2Si_{(p)}/AA332$  composite are controlled by several factors such as volume of shrinkage, distribution of binary eutectic ( $Al+Mg_2Si$ ), size of  $Mg_2Si$  particles, and intermetallic phases.

### 3.4 Tensile properties

The tensile properties of  $Mg_2Si_{(p)}/AA332$  composite shown in Fig. 7(a) consist of as cast and 5, 10, 15 and 20 wt% of  $Mg_2Si$ . Adding  $Mg_2Si$  introduced harmful effects on the toughness of the material. A typical stress-strain curve of 15%  $Mg_2Si$  was similar to the brittle materials and showed poor ductility. It is apparent that the sample of 15%  $Mg_2Si$ , which was brittle and showing poor ductility, were due to the Fe-rich intermetallic in the microstructure (Fig. 3(d)). Hurtalova *et al.* (2012) reported that a dominant Fe-rich phase such as  $\beta-Al_5FeSi$  and  $\alpha-Al_{15}(FeMn)_3Si_2$  can negatively affect the mechanical properties of materials especially ductility. In addition, the highest UTS and elongation (El) values are related to 10%  $Mg_2Si$ .

Fig. 7(b) presents the variation of UTS and elongation of the as cast and  $Mg_2Si_{(p)}/AA332$  composite. In agreement with the microstructural investigation, due to the presence of the Cu-rich intermetallic, the highest UTS and elongation was present in the 10%  $Mg_2Si$  sample. As it is known, Cu produces  $Q-Al_5Cu_2Mg_3Si_6$  and  $\theta-Al_2Cu$  precipitates, which increase overall matrix strength.

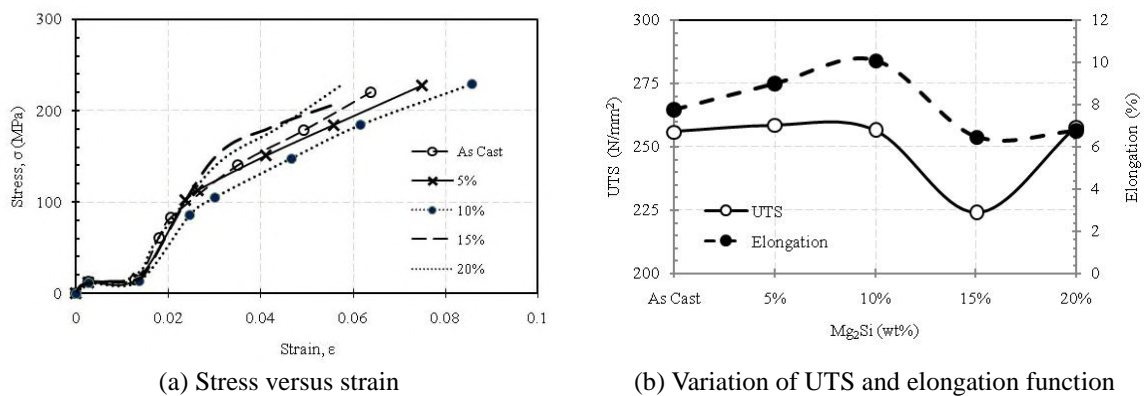


Fig. 7 Tensile properties of as cast and  $Mg_2Si_{(p)}/AA332$  composite

Table 2 Tensile properties of as cast and Mg<sub>2</sub>Si<sub>(p)</sub>/AA332 composite

	UTS (MPa)	Elongation, El (%)	Q.I
As Cast	255.793	7.727	388.99
5% Mg <sub>2</sub> Si	258.47	8.95	401.27
10% Mg <sub>2</sub> Si	256.40	10.07	406.83
15% Mg <sub>2</sub> Si	223.94	6.46	345.49
20% Mg <sub>2</sub> Si	257.87	6.73	382.08

In engineering application, the combination of UTS and elongation values is a dependable parameter in quantifying tensile properties. Hence to quantify the overall tensile properties, the quality index (Q.I.) was used. Q.I. is explained as a semi-logarithmic plot of UTS versus the elongation to fracture (El), expressed as follows (Emamy *et al.* 2013)

$$Q.I = UTS (MPa) + 150 \log(\% El) \quad (4)$$

The UTS, elongation (El), and the quality index (Q.I.) for as cast and each Mg<sub>2</sub>Si<sub>(p)</sub>/AA332 composites are listed in Table 2. Highest Q.I was achieved in the sample of 10% Mg<sub>2</sub>Si. This is similar to the microstructural characterisation (Fig. 3c), lowest density (Fig. 5a), and highest hardness (Fig. 6). Combined with AA332, the amount of 10% Mg<sub>2</sub>Si exhibited a suitable reinforcement quantity, and this is because 10% Mg<sub>2</sub>Si is close to the pseudo eutectic of Al-Mg<sub>2</sub>Si (Fig. 1). A content of Mg<sub>2</sub>Si close to pseudo eutectic (13.9 wt%) had produced tiny Mg<sub>2</sub>Si dendrite, decreased the brittle interaction, and enhanced mechanical properties such as hardness and tensile properties.

#### 4. Conclusions

The microstructural, porosity, and mechanical properties of Mg<sub>2</sub>Si<sub>(p)</sub>/AA332 containing 5, 10, 15 and 20 wt% of Mg<sub>2</sub>Si were investigated. The following conclusions were drawn:

- The microstructure of Mg<sub>2</sub>Si<sub>(p)</sub>/AA332 consisted of  $\alpha$ -Al, binary eutectic (Al+Mg<sub>2</sub>Si), Mg<sub>2</sub>Si particles, and intermetallic compound.

- The intermetallic compounds were identified as  $\theta$ -Al<sub>2</sub>Cu, Q-Al<sub>5</sub>Cu<sub>2</sub>Mg<sub>3</sub>Si<sub>6</sub>,  $\beta$ -Al<sub>3</sub>FeSi, and  $\alpha$ -Al<sub>15</sub>(FeMn)<sub>3</sub>Si<sub>2</sub>.  $\theta$ -Al<sub>2</sub>Cu forming like polygonal or blocky Q-Al<sub>5</sub>Cu<sub>2</sub>Mg<sub>3</sub>Si<sub>6</sub> appeared as “Chinese script”.  $\beta$ -Al<sub>3</sub>FeSi and  $\alpha$ -Al<sub>15</sub>(FeMn)<sub>3</sub>Si<sub>2</sub> appeared as needle-like and polyhedrons or “skeleton like respectively.

- The porosity of Mg<sub>2</sub>Si<sub>(p)</sub>/AA332 composite increased from 8 - 10% from as-cast. Meanwhile, the density decrease was in parallel with the increase of Mg<sub>2</sub>Si, (9 - 12%). Low density was detected from the sample containing 10% Mg<sub>2</sub>Si.

- The hardness of Mg<sub>2</sub>Si<sub>(p)</sub>/AA332 composite was a significant increase from 42 - 53 % from as-cast. The sample of 5% Mg<sub>2</sub>Si recorded the highest hardness (53.3%) and the sample of 15% Mg<sub>2</sub>Si recorded the lowest hardness.

- The highest UTS, elongation (El), and maximum Q.I were achieved in the sample of 10% Mg<sub>2</sub>Si.

## Acknowledgments

The research described in this paper was financially supported by the Malaysian Ministry of Higher Education (HLP Scholarship). The authors would like to thank Universiti Malaysia Perlis, Dr. Khairul Rafezi Ahmad, Dr. Ruslizam Daud, and Prof. Dr. Azmi Rahmat for their kind assistance in this research.

## References

- Alam, M.F. (2013), "Squeeze casting as alternative fabrication process for carbon fiber reinforced aluminium matrix composites", Ph.D. dissertation, Université d'Ottawa/University of Ottawa.
- Ammar, H.R., Samuel, A.M. and Samuel, F.H. (2008), "Porosity and the fatigue behavior of hypoeutectic and hypereutectic aluminum–silicon casting alloys", *Int. J. Fatigue*, **30**(6), 1024-1035.
- ASTM International E384-11 (2011), *Standard test method for Knoop and Vickers hardness of materials*, (ASTM Book of Standards), American Society for Testing and Materials, Philadelphia, USA.
- ASTM International E8/E8M (2013), *Standard test methods for tension testing of metallic materials*, (Annual Book of ASTM Standards), American Society for Testing and Materials, Philadelphia, USA.
- Aydin, M. and Findik, F. (2010), "Wear properties of magnesium matrix composites reinforced with SiO<sub>2</sub> particles", *Ind. Lubric. Tribol.*, **62**(4), 232-237.
- Belov, N.A., Eskin, D.G. and Avxentieva, N.N. (2005), "Constituent phase diagrams of the Al–Cu–Fe–Mg–Ni–Si system and their application to the analysis of aluminium piston alloys", *Acta Mater.*, **53**(17), 4709-4722.
- Black, J.T. and Kohser, R.A. (2008), *Materials and processes in manufacturing*, (10th Ed.), John Wiley & Sons, Inc, USA.
- Dhanashekar, M. and Kumar, V.S. (2014), "Squeeze casting of aluminium metal matrix composites-an overview", *Procedia Eng.*, **97**, 412-420.
- Emamy, M., Yeganeh, S.V., Razaghian, A. and Tavighi, K. (2013), "Microstructures and tensile properties of hot-extruded Al matrix composites containing different amounts of Mg<sub>2</sub>Si", *Mater. Sci. Eng.: A*, **586**, 190-196.
- Farkoosh, A.R. and Pegguleryuz, M. (2015), "Enhanced mechanical properties of an Al–Si–Cu–Mg alloy at 300° C: Effects of Mg and the Q-precipitate phase", *Mater. Sci. Eng.: A*, **621**, 277-286.
- Garza-Delgado, A. (2007), "A study of casting distortion and residual stresses in die casting", Ph.D. Dissertation, Ohio State University.
- Hadian, R., Emamy, M. and Campbell, J. (2009), "Modification of cast Al–Mg<sub>2</sub>Si metal matrix composite by Li", *Metall Mater Trans B*, **40**(6), 822-832.
- Hamedan, A.D. and Shahmiri, M. (2012), "Production of A356–1wt% SiC nanocomposite by the modified stir casting method", *Mater. Sci. Eng. A*, **556**, 921-926.
- Hosseini, V.A., Shabestari, S.G. and Gholizadeh, R. (2013), "Study on the effect of cooling rate on the solidification parameters, microstructure, and mechanical properties of LM13 alloy using cooling curve thermal analysis technique", *Mater. Des.*, **50**, 7-14.
- Hurtalová, L., Tillová, E. and Chalupová, M. (2012), "Identification and analysis of intermetallic phases in age-hardened recycled AlSi9Cu3 cast alloy", *Arch. Mech. Eng.*, **59**(4), 385-396.
- Kumar, K.A., Pillai, U.T.S., Pai, B.C. and Chakraborty, M. (2013), "Dry sliding wear behaviour of Mg–Si alloys", *Wear*, **303**(1), 56-64.
- Liu, Z., Liu, X.M. and Xie, M. (2011), "Effect of Mg<sub>2</sub>Si contents on microstructure of Mg<sub>2</sub>Si particle reinforced hypereutectic Al–Si alloy composites", *Appl. Mech. Mater.*, **66**, 160-163, Trans Tech Publications.
- Mandal, A. and Makhlof, M.M. (2009), "Development of a novel hypereutectic aluminum–siliconmagnesium alloy for die casting", *Transact. Ind. Inst. Metals*, **62**(4-5), 357-360.

- Mitrasinovic, A. (2004), "Development of thermal analysis and analytical techniques for the assessment of porosity and metallurgical characteristics in 3XX aluminum alloys", Ph.D. Dissertation, University of Windsor.
- Mrowka-Nowotnik, G. (2011), "Intermetallic phases examination in cast AlSi5Cu1Mg and AlCu4Ni2Mg2 aluminium alloys in as-cast and T6 condition, recent trends in processing and degradation of aluminium alloys", April.
- Nasiri, N., Emamy, M. and Malekan, A. (2012), "Microstructural evolution and tensile properties of the in situ Al-15% Mg 2 Si composite with extra Si contents", *Mater. Des.*, **37**, 215-222.
- Okayasu, M., Ohkura, Y., Takeuchi, S., Takasu, S., Ohfuji, H. and Shiraishi, T. (2012), "A study of the mechanical properties of an Al-Si-Cu alloy (ADC12) produced by various casting processes", *Mater. Sci. Eng.: A*, **543**, 185-192.
- Panwar, R.S. and Pandey, O.P. (2013), "Analysis of wear track and debris of stir cast LM13/Zr composite at elevated temperatures", *Mater Charact.*, **75**, 200-213.
- Qiang, Z. (2009), "Development of hybrid Mg-based composites", Ph.D. Dissertation, University of Windsor, Ontario, Canada.
- Sajjadi, S.A., Ezatpour, H.R. and Parizi, M.T. (2012), "Comparison of microstructure and mechanical properties of A356 aluminum alloy/Al<sub>2</sub>O<sub>3</sub> composites fabricated by stir and compo-casting processes", *Mater. Des.*, **34**, 106-111.
- Samuel, E., Samuel, A.M., Doty, H.W., Valtierra, S. and Samuel, F.H. (2014), "Intermetallic phases in Al-Si based cast alloys: new perspective", *Int. J. Cast Metal. Res.*, **27**(2), 107-114.
- Sekar, K., Allesu, K. and Joseph, M.A. (2013), "Microstructure, double shear and tribological properties of A356 aluminum alloy fabricated by gravity, vacuum and squeeze casting method", *Int. J. Mech. Struct.*, **4**(1), 25-34.
- Sharma, P., Chauhan, G. and Sharma, N. (2011), "Production of AMC by stir casting—an overview", *Int. J. Contemporary Practices*, **2**(1), 23-46.
- Soltani, N., Nodooshan, H.J., Bahrami, A., Pech-Canul, M.I., Liu, W. and Wu, G. (2014), "Effect of hot extrusion on wear properties of Al-15wt.% Mg 2 Si in situ metal matrix composites", *Mater. Des.*, **53**, 774-781.
- Tang, S.Q., Zhou, J.X., Tian, C.W. and Yang, Y.S. (2011), "Morphology modification of Mg 2 Si by Sr addition in Mg-4% Si alloy", *Transactions of Nonferrous Metal. Soc. China*, **21**(9), 1932-1936.
- Taylor, J.A. (2012), "Iron-containing intermetallic phases in Al-Si based casting alloys", *Procedia Mater. Sci.*, **1**, 19-33.
- Valibeygloo, N., Khosroshahi, R.A. and Mousavian, R.T. (2013), "Microstructural and mechanical properties of Al-4.5 wt% Cu reinforced with alumina nanoparticles by stir casting method", *Int. J. Minerals, Metall. Mater.*, **20**(10), 978-985.
- Vijeesh, V. and Prabhu, K.N. (2014), "Review of microstructure evolution in hypereutectic Al-Si alloys and its effect on wear properties", *Transactions Ind. Inst. Metal.*, **67**(1), 1-18.
- Williams, D. (2012), "Composites in cars making vehicles lighter, safer and more fuel-efficient", Mechanical Engineering University of Utah. Retrieved October, 2013.
- Wu, X.F., Zhang, G.G. and Wu, F.F. (2013), "Microstructure and dry sliding wear behavior of cast Al-Mg<sub>2</sub>Si in-situ metal matrix composite modified by Nd", *Rare Metal.*, **32**(3), 284-289.
- Yıldırım, M. and Özyürek, D. (2013), "The effects of Mg amount on the microstructure and mechanical properties of Al-Si-Mg alloys", *Mater. Des.*, **51**, 767-774.
- Yu, H. (2010), "Processing routes for aluminum based", Ph.D. Dissertation, Worcester Polytechnic Institute.
- Zeren, M. (2007), "The effect of heat-treatment on aluminum-based piston alloys", *Mater. Des.*, **28**(9), 2511-2517.